J|A|C|S
ARTICLES
Published on Web 03/13/2003

Membrane Insertion of a Lipidated Ras Peptide Studied by FTIR, Solid-State NMR, and Neutron Diffraction Spectroscopy†

Daniel Huster,*,‡ Alexander Vogel,‡ Catherine Katzka,§ Holger A. Scheidt,‡ Hans Binder,⊥ Silvia Dante,|| Thomas Gutberlet,|| Olaf Zschörnig,▽ Herbert Waldmann,§ and Klaus Arnold▽

Contribution from the Junior Research Group "Solid-state NMR Studies of Membrane-associated Proteins" and Institute of Medical Physics and Biophysics, University of Leipzig, Liebigstrasse 27, D-04103 Leipzig, Germany, Max Planck Institute of Molecular Physiology, Otto-Hahn-Strasse 11, D-44227 Dortmund, Germany, Interdisciplinary Center for Bioinformatics of the University of Leipzig, Kreutzstrasse 7b, D-04103 Leipzig, Germany, and Hahn Meitner Institute Berlin GmbH, Glienicker Strasse 100, D-14109 Berlin, Germany

Received October 14, 2002; E-mail: husd@medizin.uni-leipzig.de

Abstract: Membrane binding of a doubly lipid modified heptapeptide from the C-terminus of the human N-ras protein was studied by Fourier transform infrared, solid-state NMR, and neutron diffraction spectroscopy. The 16:0 peptide chains insert well into the 1,2-dimyristoyl-*sn*-glycero-3-phosphocholine phospholipid matrix. This is indicated by a common main phase transition temperature of 21.5 °C for both the lipid and peptide chains as revealed by FTIR measurements. Further, ^{2}H NMR reveals that peptide and lipid chains have approximately the same chain length in the liquid crystalline state. This is achieved by a much lower order parameter of the 16:0 peptide chains compared to the 14:0 phospholipid chains. Finally, proton/deuterium contrast variation of neutron diffraction experiments indicates that peptide chains are localized in the membrane interior analogous to the phospholipid chains. In agreement with this model of peptide chain insertion, the peptide part is localized at the lipid−water interface of the membrane. This is revealed by ^{1}H nuclear Overhauser enhancement spectra recorded under magic angle spinning conditions. Quantitative cross-peak analysis allows the examination of the average location of the peptide backbone and side chains with respect to the membrane. While the backbone shows the strongest cross-relaxation rates with the phospholipid glycerol, the hydrophobic side chains of the peptide insert deeper into the membrane interior. This is supported by neutron diffraction experiments that reveal a peptide distribution in the lipid−water interface of the membrane. Concurring with these experimental findings, the amide protons of the peptide show strong water exchange as seen in NMR and FTIR measurements. No indications for a hydrogen-bonded secondary structure of the peptide backbone are found. Therefore, membrane binding of the C-terminus of the N-ras protein is mainly due to lipid chain insertion but also supported by interactions between hydrophobic side chains and the lipid membrane. The peptide assumes a mobile and disordered conformation in the membrane. Since the C-terminus of the soluble part of the ras protein is also disordered, we hypothesize that our model for membrane binding of the ras peptide realistically describes the membrane binding of the lipidated C-terminus of the active ras protein.

Introduction

Fatty acid modifications represent a common structural feature of membrane binding of proteins involved in signal transduction events of the cell.[1−5] A typical example for a lipid-modified membrane-binding protein is the GTPase ras. Ras proteins are mediators in the signal cascade from receptor tyrosine kinases to the cell nucleus by activating downstream effectors to stimulate cell proliferation or differentiation.[6−9] Malfunction of these regulators can lead to uncontrolled cell growth and finally

* Address correspondence to this author. Phone: +49 (0) 341 97 15706. Fax.: +49 (0) 341 97 15709.

† Abbreviations: BPTI, bovine pancreatic trypsin inhibitor; COG, center of gravity; DMPC, 1,2-dimyristoyl-*sn*-glycero-3-phosphocholine; DMPC-d_{54}, 1,2-dimyristoyl-d_{54}-*sn*-glycero-3-phosphocholine; DMPC-d_{67}, 1,2-dimyristoyl-d_{54}-*sn*-glycero-3-phosphocholine-1,1,2,2-d_4-*N*,*N*,*N*-trimethyl-d_9; MAPK, mitogen-activated protein kinase; MAS, magic angle spinning; MARCKS, myristoylated alanine-rich C kinase substrate; NOESY, nuclear Overhauser enhancement spectroscopy; ATR, attenuated total reflection.

‡ Junior Research Group "Solid-state NMR Studies of Membrane-associated Proteins", University of Leipzig.

§ Max Planck Institute of Molecular Physiology.

⊥ Interdisciplinary Center for Bioinformatics of the University of Leipzig.

|| Hahn Meitner Institute Berlin GmbH.

▽ Institute of Medical Physics and Biophysics, University of Leipzig.

(1) Reuther, G. W.; Der, C. J. *Curr. Opin. Cell Biol.* **2000**, *12*, 157−165.
(2) Casey, P. J. *Science* **1995**, *268*, 221−225.
(3) Schafer, W. R.; Rine, J. *Annu. Rev. Genet.* **1992**, *26*, 209−237.
(4) Clarke, S. *Annu. Rev. Biochem.* **1992**, *61*, 355−386.
(5) Gelb, M. H. *Science* **1995**, *275*, 1750−1751.
(6) Wittinghofer, A.; Waldmann, H. *Angew. Chem., Int. Ed.* **2000**, *39*, 4192−4214.
(7) Shields, J. M.; Pruitt, K.; McFall, A.; Shaub, A.; Der, C. J. *Trends Cell Biol.* **2000**, *10*, 147−154.
(8) Egan, S. E.; Weinberg, R. A. *Nature* **1993**, *365*, 781−783.
(9) Boguski, M. S.; McCormick, F. *Nature* **1993**, *366*, 643−654.

10.1021/ja0289245 CCC: $25.00

cancer. It is known that about 30% of all human cancers carry a mutated form of the ras protein.

The ras protein must be associated with the plasma membrane to function; non-lipid-modified ras is cytosolic and thus inactive. By translocation to the membrane from the cytosol, the effective concentration of the protein is increased at least 1000-fold due to reduction of the dimensionality of distribution from three to two.[10] The interaction with other downstream effectors occurs only at the membrane surface. To achieve the high propensity for the plasma membrane, ras can acquire two different types of lipid modifications in a series of post-translational modifications.[11,12] For instance, in N-ras, first, Cys 186 is farnesylated and then Cys 181 is palmitoylated. Two members of the ras family, H-ras and N-ras, are known to undergo this double lipid modification. Only two lipid modifications provide the protein with sufficient hydrophobic energy to bind to the plasma membrane, where it participates in the signal transduction process. Nonpalmitoylated but farnesylated H- or N-ras molecules mislocate to the cytosol and break the signal cascade.[13]

In recent years several biophysical studies have shed light on how the distribution of lipidated proteins is regulated between a membrane-associated state, where the protein actively participates in biological functions, and a translocated cytosolic state, where the protein is inactive.[14] The thermodynamics of membrane binding was investigated in model systems consisting of artificial membranes and lipid-modified peptides. These studies revealed that a single lipid modification provides insufficient binding energy to permanently anchor the peptide to the membrane, leading to a fast equilibrium between an adsorbed state and a desorbed state with typical half-life times on the order of seconds.[15,16] However, an additional lipid modification leads to permanent peptide partitioning into the membrane with average half-life times on the order of hours to days.[17,18] This supports the biological finding that nonpalmitoylated ras fails to activate mitogen-activated protein kinase (MAPK) in the downstream regulation of signal transduction events.[13]

Alternatively to double lipid modification, stable association of peptides with a single lipid modification in negatively charged membranes is observed for peptides carrying a cluster of basic amino acids such as the myristoylated alanine-rich C kinase substrate (MARCKS), pp60^{src} (Src), or K-ras.[19−25] In this case, electrostatic attraction between negatively charged phospholipid headgroups and a cluster of positively charged amino acid residues of the peptides provides additional electrostatic binding energy and prevents the peptide from desorption to the aqueous phase.

Unlike membrane proteins that are permanently anchored to the plasma membrane by transmembrane α-helices or β-barrel structures, membrane association by post-translational lipid modification is a reversible process: the palmitoyl moiety can be hydrolyzed, leading to a desorption of the protein from the plasma membrane.[26,27] Alternatively, amino acids in the basic domain of singly lipid modified proteins can be phosphorylated by kinases, leading to a reduction of the electrostatic attraction and finally to the desorption of the protein from the membrane surface.[28,29] Such a dynamic regulation of membrane partitioning is found for a variety of lipidated proteins such as ras, MARCKS, Src, recoverin, and others.

While the structure of the soluble part of the ras protein (residues 1−166) has been solved by both X-ray diffraction[30−32] and solution NMR spectroscopy,[33] little is known about the structure, dynamics, and details of membrane association of the membrane-binding C-terminus. Therefore, in this study, we investigate membrane binding of a doubly lipid modified synthetic heptapeptide mimicking the C-terminus of the human N-ras protein (residues 180−186). Using a variety of biophysical methods, we address the following two questions: Where are the peptide backbone and side chains localized in the membrane, and what is their dynamic transversal distribution? How do the lipid chains of the peptide insert into the host phospholipid bilayer?

In a preliminary qualitative investigation, we have investigated aqueous suspensions of the ras peptide and 1,2-dimyristoyl-*sn*-glycero-3-phosphocholine (DMPC) multilamellar vesicles by ^{1}H magic angle spinning (MAS) nuclear Overauser enhancement spectroscopy (NOESY) and found cross-peaks between peptide side chains and phospholipid chain signals.[34] This suggests that the peptide penetrates the lipid−water interface of the membrane and interacts with the upper segments of the hydrocarbon chains. Here, we have applied attenuated total reflection Fourier transform infrared spectroscopy (ATR FTIR), quantitative ^{1}H MAS NOESY, ^{2}H solid-state NMR spectroscopy, and neutron diffraction techniques to study the localization of the C-terminus of the human N-ras protein in the membrane to quantitatively determine the peptide distribution in the membrane.

Materials and Methods

Materials. The lipids DMPC, 1,2-dimyristoyl-d_{54}-*sn*-glycero-3-phosphocholine (DMPC-d_{54}), and 1,2-dimyristoyl-d_{54}-*sn*-glycero-3-phosphocholine-1,1,2,2-d_4-*N*,*N*,*N*-trimethyl-d_9 (DMPC-d_{67}) were pur-

(10) Murray, D.; Ben-Tal, N.; Honig, B.; McLaughlin, S. *Structure* **1997**, *5*, 985−989.
(11) Hancock, J. F.; Magee, A. I.; Childs, J. E.; Marshall, C. J. *Cell* **1989**, *57*, 1167−1177.
(12) Hancock, J. F.; Paterson, H.; Marshall, C. J. *Cell* **1990**, *63*, 133−139.
(13) Dudler, T.; Gelb, M. H. *J. Biol. Chem.* **1996**, *271*, 11541−11547.
(14) Silvius, J. R. Lipidated peptides as tools for understanding the membrane interactions of lipid-modified proteins. In *Peptide Lipid*; Simon, S. A., McIntosh, T. J., Eds.; Elsevier: New York, 2002; pp 371−395.
(15) Peitzsch, R. M.; McLaughlin, S. *Biochemistry* **1993**, *32*, 10436−10443.
(16) Silvius, J. R.; l'Heureux, F. *Biochemistry* **1994**, *33*, 3014−3022.
(17) Shahinian, S.; Silvius, J. R. *Biochemistry* **1995**, *34*, 3813−3822.
(18) Schroeder, H.; Leventis, R.; Rex, S.; Schelhaas, M.; Nagele, E.; Waldmann, H.; Silvius, J. R. *Biochemistry* **1997**, *36*, 13102−13109.
(19) Buser, C. A.; Sigal, C. T.; Resh, M. D.; McLaughlin, S. *Biochemistry* **1994**, *33*, 13093−13101.
(20) Leventis, R.; Silvius, J. R. *Biochemistry* **1998**, *37*, 7640−7648.
(21) Sigal, C. T.; Zhou, W.; Buser, C. A.; McLaughlin, S.; Resh, M. D. *Proc. Natl. Acad. Sci. U.S.A.* **1994**, *91*, 12253−12257.
(22) Murray, D.; Hermida-Matsumoto, L.; Buser, C. A.; Tsang, J.; Sigal, C. T.; Ben-Tal, N.; Honig, B.; Resh, M. D.; McLaughlin, S. *Biochemistry* **1998**, *37*, 2145−2159.
(23) Qin, Z.; Cafiso, D. S. *Biochemistry* **1996**, *35*, 2917−2925.
(24) Victor, K.; Cafiso, D. S. *Biochemistry* **1998**, *37*, 3402−3410.
(25) Vergeres, G.; Manenti, S.; Weber, T.; Sturzinger, C. *J. Biol. Chem.* **1995**, *270*, 19879−19887.
(26) Wilson, P. T.; Bourne, H. R. *J. Biol. Chem.* **1995**, *270*, 9667−9675.
(27) Hinterding, K.; Alonso-Diaz, D.; Waldmann, H. *Angew. Chem., Int. Ed.* **1998**, *37*, 688−749.
(28) McLaughlin, S.; Aderem, A. *Trends Biochem. Sci.* **1995**, *20*, 272−276.
(29) Bhatnagar, R. S.; Gordon, J. I. *Trends Cell Biol.* **1997**, *7*, 14−20.
(30) Milburn, M. V.; Tong, L.; deVos, A. M.; Brunger, A.; Yamaizumi, Z.; Nishimura, S.; Kim, S. H. *Science* **1990**, *247*, 939−945.
(31) Krengel, U.; Schlichting, L.; Scherer, A.; Schumann, R.; Frech, M.; John, J.; Kabsch, W.; Pai, E. F.; Wittinghofer, A. *Cell* **1990**, *62*, 539−548.
(32) Pai, E. F.; Kabsch, W.; Krengel, U.; Holmes, K. C.; John, J.; Wittinghofer, A. *Nature* **1989**, *341*, 209−214.
(33) Kraulis, P. J.; Domaille, P. J.; Campbell-Burk, S. L.; Van Aken, T.; Laue, E. D. *Biochemistry* **1994**, *33*, 3515−3531.
(34) Huster, D.; Kuhn, K.; Kadereit, D.; Waldmann, H.; Arnold, K. *Angew. Chem., Int. Ed.* **2001**, *40*, 1056−1058.

chased from Avanti Polar Lipids, Inc. (Alabaster, AL) and used without further purification. Protected amino acids and coupling reagents were obtained from Novabiochem (La Jolla, CA), and d_{33} isotopically labeled hexadecyl alcohol was obtained from Isotec (Miamisburg, OH).

The ras peptide with an amino acid sequence of H-Gly-Cys(R^1)-Met-Gly-Leu-Pro-Cys(R^2)-OMe was synthesized as described in refs 27, 35, and 36 and is briefly outlined below. R^1 and R^2 indicate the lipid modifications. In the first ras peptide investigated in this study, R^1 represents a palmitic (Pal) and R^2 a hexadecyl (HD) thioether modification; for the second ras peptide both R^1 and R^2 are deuterated hexadecyl-d_{33} thioether modifications. In the following these peptides are abbreviated ras and ras-d_{66}, respectively.

Peptide Synthesis. The peptides H-Gly-Cys(R^1)-Met-Gly-Leu-Pro-Cys(R^2)-OMe were modularly assembled in solution from three building blocks: Boc-Gly-Cys(R^1)-OH, Boc-Met-Gly-Leu-Pro-OH, and H-Cys-(R^2)-OMe. H-Cys(R^1)-OMe was synthesized in solution starting from the hexadecylation of H-Cys-OMe·HCl using previously described methods,[37] and then coupled in solution to Boc-Met-Gly-Leu-Pro-OH[38] using carbodiimide methods. After acid-mediated cleavage of the Boc group, H-Met-Gly-Leu-Pro-Cys(R^2)-OMe was coupled to Boc-Gly-Cys-(R^1)-OH using carbodiimide methods. Final TFA-mediated deprotection of the Boc group afforded the desired peptide in decent yields. The building block Boc-Gly-Cys(R^1)-OH was synthesized starting from bis-Boc-protected (glycylcystine) bis(allyl ester) by cleavage of the disulfide bond with dithiothreitol and lipidation with either palmitoyl chloride or hexadecyl-d_{33} iodide, synthesized from hexadecyl-d_{33} alcohol via an Appel reaction (1.3 equiv of PPh_3, 1 equiv of I_2, 1.5 equiv of imidazole), following a previously described method,[39] respectively, in the case of the unlabeled and labeled peptides. By means of these methods the following peptides were synthesized: H-Gly-Cys(Pal)-Met-Gly-Leu-Pro-Cys(HD)-OMe and H-Gly-Cys(HD-d_{33})-Met-Gly-Leu-Pro-Cys(HD-d_{33})-OMe.

FTIR Measurements. For FTIR measurements, aliquots of lipid and peptide were mixed in chloroform and spread on a ZnSe ATR crystal (70 × 10 × 5 mm^3 trapezoid, face angle 45°, six active reflections). While drying, the sample was spread uniformly over an area of $A_{film} \approx 40 \times 7$ mm^2 onto the crystal surface by gently stroking with the syringe tip. The mean film thickness was approximately 3 μm.

The ATR crystal was mounted into a horizontal ATR holder (Graseby Specac, Kent, U.K.) which was modified to adjust the hydration degree of the sample.[40,41] The film was hydrated to excess D_2O using a wet sponge placed within the sealed sample chamber. Polarized absorbance spectra, $A_{\parallel}(\nu)$ and $A_{\perp}(\nu)$ (128 scans, nominal resolution 2 cm^{-1}), were recorded using a BioRad FTS-60a Fourier transform infrared spectrometer (Digilab, Massachusetts) at two perpendicular polarizations of the IR beam, parallel ($\parallel$) and perpendicular ($\perp$) with respect to the plane of incidence. The peak positions and the center of gravity (COG) of the absorption bands were determined from the weighted sum spectrum

$$A(\nu) = A_{\parallel}(\nu) + K_2^{\infty} A_{\perp}(\nu)$$

The IR order parameter of an absorption band was calculated from the dichroic ratio of the integral, baseline-corrected polarized absorbances, $R = A_{\parallel}/A_{\perp}$, using Harricks thick film approximation[42] (see also reference 41 for details):

$$S_{IR} = (R - 2)/(R + 2.55) \quad (1)$$

The molecular ordering of the hydrocarbon chains can be estimated by means of the longitudinal chain order parameter using the IR order parameters of the symmetric and antisymmetric CH_2 or CD_2 stretching bands, $S_{IR}(\nu_s)$ and $S_{IR}(\nu_{as})$, respectively:[43,44]

$$S_{\theta} = -(S_{IR}(\nu_s) + S_{IR}(\nu_{as})) \quad (2)$$

It provides a measure of the mean segmental order and of the mean tilt of the chain axes with respect to the bilayer normal.

^{1}H Magic Angle Spinning NMR. Aliquots of phospholipid and peptide (molar ratio of 10:1) were combined in methanol, dried under a stream of nitrogen, and dissolved in cyclohexane. After being frozen in liquid nitrogen, the samples were lyophilized under a vacuum of approximately 0.1 mbar. Subsequently, the sample was hydrated to 30 wt % H_2O, freeze−thawed, stirred, gently centrifuged for equilibration, and transferred to spherical inserts for 4 mm MAS rotors.

^{1}H MAS NMR experiments were carried out on a Bruker DRX600 spectrometer (Bruker BioSpin, Rheinstetten, Germany) operating at a resonance frequency of 600.13 MHz for ^{1}H at a temperature of 37 °C. The MAS spinning frequency was 12 kHz. Spectra were acquired with a spectrum width of 10.9 kHz and a typical 90° pulse length of 6.2 μs. Two-dimensional NOESY experiments[45] were carried out with phase cycling in the States-TPPI mode with a mixing time of 200 ms. A total of 400 complex data points were collected in the indirect dimensions with 32 transients per increment with a relaxation delay of 4 s between successive scans, yielding a total acquisition time of approximately 15 h. A Gaussian window function was used for processing in both dimensions.

Peak volumes in the 2D NOESY spectrum were fitted to a three-dimensional Gaussian peak shape using the SigmaPlot software package (Jandel Scientific Software, San Rafael, CA). Cross-relaxation rates (σ_{ij}) were calculated according to[46]

$$\sigma_{ij} = \frac{A_{ij}(t_m)}{A_{jj}(t_m)t_m} \quad (3)$$

The variable $A_{ij}(t_m)$ represents the cross-peak volume at mixing time t_m and $A_{jj}(t_m)$ the diagonal peak volume at mixing time zero.

^{2}H and ^{31}P Solid-State NMR. For static NMR measurements, samples were prepared analogous to the ^{1}H NMR samples, except that the hydration was carried out with deuterium-depleted H_2O. After equilibration, samples were filled into 5 mm glass vials, and the vials were sealed for NMR measurements.

^{2}H NMR spectra were recorded on a Bruker DSX400 NMR spectrometer operating at a resonance frequency of 61.48 MHz for ^{2}H using a double-channel solids probe equipped with a 5 mm solenoid coil. The ^{2}H spectra were accumulated at a spectrum width of 200 kHz using a phase-cycled quadrupolar echo sequence[47] and a relaxation delay of 400 ms. The two 3.5 μs $\pi/2$ pulses were separated by a 50 μs delay. Spectra were left shifted after acquisition to start Fourier transformation on top of the quadrupolar echo. A 100 Hz exponential line broadening was applied.

The ^{2}H NMR powder spectra were depaked[48] using the algorithm of McCabe and Wassall,[49] and smoothed order parameter profiles[50] were

(35) Schelhaas, M.; Glomsda, S.; Hänsler, M.; Jakubke, H.-D.; Waldmann, H. *Angew. Chem., Int. Ed. Engl.* **1996**, *35*, 106−109.
(36) Nägele, E.; Schelhaas, M.; Kuder, N.; Waldmann, H. *J. Am. Chem. Soc.* **1998**, *120*, 6889−6902.
(37) Xue, C. B.; Becker, J.; Naider, F. *Int. J. Pept. Protein Res.* **1991**, *37*, 476−487.
(38) Kuhn, K. 1999. Ph.D. Thesis, University of Karlsruhe, Germany.
(39) Appel, R. *Angew. Chem., Int. Ed. Engl.* **1975**, *14*, 801−810.
(40) Binder, H.; Anikin, A.; Kohlstrunk, B.; Klose, G. *J. Phys. Chem. B* **1997**, *101*, 6618−6628.
(41) Binder, H. *Appl. Spectrosc. Rev.* **2003**, *38*, 15−69.
(42) Harrick, N. J. *Internal Reflection Spectroscopy*; John Wiley & Sons: New York, 1967.
(43) Binder, H.; Gawrisch, K. *J. Phys. Chem. B* **2001**, *105*, 12378−12390.
(44) Binder, H.; Schmiedel, H. *Vib. Spectrosc.* **1999**, *21*, 51−73.
(45) Jeener, J.; Meier, B. H.; Bachmann, P.; Ernst, R. R. *J. Chem. Phys.* **1979**, *71*, 4546−4553.
(46) Huster, D.; Arnold, K.; Gawrisch, K. *J. Phys. Chem. B* **1999**, *103*, 243−251.
(47) Davis, J. H.; Jeffrey, K. R.; Bloom, M.; Valic, M. I.; Higgs, T. P. *Chem. Phys. Lett.* **1976**, *42*, 390−394.
(48) Sternin, E.; Bloom, M.; MacKay, L. *J. Magn. Reson.* **1983**, *55*, 274−282.
(49) McCabe, M. A.; Wassall, S. R. *J. Magn. Reson., B* **1995**, *106*, 80−82.

determined from the observed quadrupolar splittings ($\Delta\nu_Q$) according to

$$\Delta\nu_Q = \frac{3}{4}\frac{e^2qQ}{h}S(n) \quad (4)$$

where e^2qQ/h represents the quadrupolar coupling constant (167 kHz for ^{2}H in the C$-^2$H bond) and $S(n)$ the chain order parameter for the nth carbon position in the chain. Details of the order parameter determination have been outlined in ref 51.

Static ^{31}P NMR experiments were carried out on a Bruker DSX400 NMR spectrometer at a resonance frequency of 162.12 MHz using the same 5 mm probe. ^{31}P spectra were acquired using a Hahn-echo pulse sequence with a delay between pulses of 50 μs, a 90° pulse length of 5 μs, a spectral with of 125 kHz, and a recycle delay of 1 s. Broadband ^{1}H decoupling was applied during signal acquisition.

Neutron Diffraction. For neutron diffraction measurements, aliquots of phospholipid and the ras or ras-d_{66} peptide were mixed at a molar ratio of 10:1 in chloroform. The chloroform solution was sprayed onto quartz plates (20 mm × 50 mm) and dried under vacuum overnight. Samples were hydrated for at least 24 h in saturated salt solution (K_2SO_4 for a relative humidity of 98%) or pure water (for a relative humidity of 100%) at room temperature. For contrast variations, H_2O, H_2O/D_2O (50:50), and D_2O solutions were used. The quartz plates were mounted onto a sample holder and sealed in a thermostated, cylindrical aluminum container, which also contained water or the saturated salt solution to ensure constant relative humidity during the experiment.

Neutron diffraction patterns were recorded on the V1 membrane diffractometer at BENSC, Hahn-Meitner-Institut, Berlin, Germany, using a wavelength of 4.5 Å. All measurements were carried out at a temperature of 30 °C.

One-dimensional scattering length density profiles were obtained by calculating the one-dimensional Fourier synthesis

$$\rho(z) = \sum_{h=1}^{h_{max}} \pm F_h \cos\left(\frac{2\pi hz}{d}\right) \quad (5)$$

where h is the order of the collected Bragg peak, d the layer thickness, and F_h the Fourier coefficient using the background-corrected maximum intensity of the corresponding Bragg peak $F_h = (Ih)^{1/2}$.[52] The sign of the Fourier coefficient was obtained from the contrast variation measurements.[53,54] Retrieved neutron scattering length density profiles were scaled to a common relative basis of zero scattering length density.

Results

ATR FTIR Measurements. In Figure 1, an ATR FTIR spectrum of DMPC-d_{67}/ras in D_2O at a molar ratio of 10:1 and a temperature of 30 °C is shown. The bands of the symmetric and antisymmetric CH_2 stretching modes of the peptide chains at 2853 and 2921 cm^{-1}, respectively, can be well separated from the band of the symmetric and antisymmetric CD_2 stretching modes of the phospholipid chains at 2095 and 2195 cm^{-1}. Thus, individual spectral information for both lipid and peptide polymethylene chains can be obtained from the same sample. Further, characteristic amide I and II bands of the peptide are resolved near 1650 and 1450 cm^{-1}, respectively. The latter mode however strongly overlaps with methylene bending vibrations of the acyl chains of the lipid. The shape of the amide I band of the ras peptide shows a broad maximum centered at 1650 cm^{-1} and a sharp peak at 1638 cm^{-1} which can be assigned to peptide molecules with a dominant fraction of amino acid residues in a disordered structure and to a small portion with residues in a H-bonded structure similar to that in a β-sheet.[55] The different intensities of the polarized spectra $A_{||}$ and $2A_\perp$ clearly reflect a nonrandom orientation of the peptides in the sample. The analysis of the linear dichroism in terms of molecular orientation will be published separately (manuscript in preparation). Additionally, substitution of the H_2O by a D_2O atmosphere shifts the amide II band from 1540 to 1450 cm^{-1} within a few minutes, indicating that the amide protons of the peptide backbone exchange with the solvent. Therefore, the peptide backbone must be well accessible by the aqueous phase.

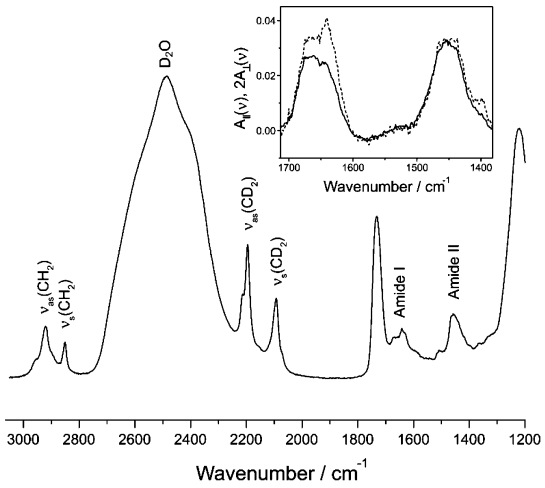

Figure 1. Attenuated total reflection FTIR spectrum of oriented bilayer stacks of DMPC-d_{67}/ras at a molar ratio of 10:1. For this sample, a D_2O atmosphere of 95% relative humidity was established, and the spectrum was acquired at 30 °C. FTIR bands of interest are assigned. The inset shows the amide bands of the spectrum after subtraction of the pure lipid spectrum at two polarizations ($A_{||}(\nu)$, solid line; $2A_\perp(\nu)$, dotted line).

Figure 2 shows the COG of the antisymmetric methylene stretching band of protonated lipid and deuterated peptide chains as a function of temperature. At the main phase transition of the lipid, the COGs of the lipid acyl chains stepwisely shift toward higher wavenumbers. The phase transition of pure DMPC-d_{67} occurs at 21.5 °C, which is slightly below the phase transition temperature of protonated DMPC near 24 °C.[56] In the presence of the ras peptide, the phase transition of DMPC-d_{67} slightly broadens but occurs at the same temperature as for the pure lipid.

The COGs of the antisymmetric stretching band of the CH_2 groups of the ras peptide chains shift toward higher wavenumbers exactly at the same temperature as the respective CD_2 band of the phospholipid chains. This effect indicates that the peptide chains undergo an order−disorder melting transition parallel to the main phase transition of DMPC. The conformational properties of the peptide chains are obviously determined by the DMPC host membrane. Consequently they must be well incorporated into the bilayer. Furthermore, a phase separation between peptide-rich and lipid-rich domains is incompatible with the observed results.

(50) Lafleur, M.; Fine, B.; Sternin, E.; Cullis, P. R.; Bloom, M. *Biophys. J.* **1989**, *56*, 1037−1041.
(51) Huster, D.; Arnold, K.; Gawrisch, K. *Biochemistry* **1998**, *37*, 17299−17308.
(52) King, G. I.; White, S. H. *Biophys. J.* **1986**, *49*, 1047−1054.
(53) Worcester, D. L.; Franks, N. P. *J. Mol. Biol.* **1976**, *100*, 359−378.
(54) Franks, N. P.; Lieb, W. R. *J. Mol. Biol.* **1979**, *133*, 469−500.
(55) Chirgadze, Y. N.; Shestopalov, B. V.; Venyaminov, S. Y. *Biopolymers* **1973**, *12*, 1337−1351.
(56) Mädler, B.; Binder, H.; Klose, G. *J. Colloid Interface Sci.* **1998**, *202*, 124−138.

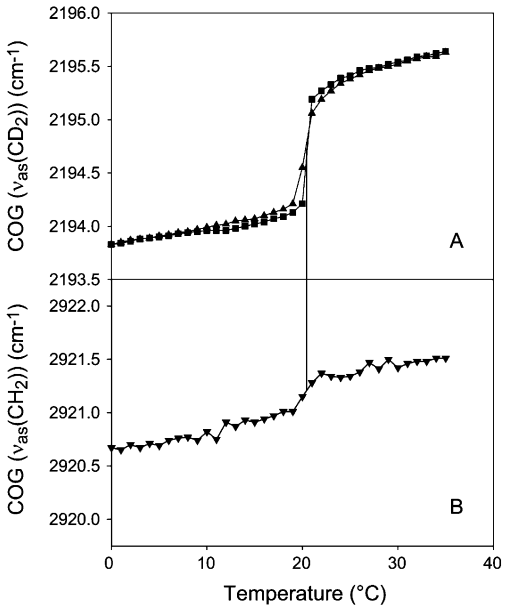

Figure 2. Wavelengths of the asymmetric methylene stretching band for pure DMPC chains (■), DMPC chains in the presence of ras at a molar ratio of 10:1 (▲), and the ras chains in the same preparation (▼). The vertical line indicates the midpoint of the phase transition. The data were acquired at full hydration (100% relative humidity).

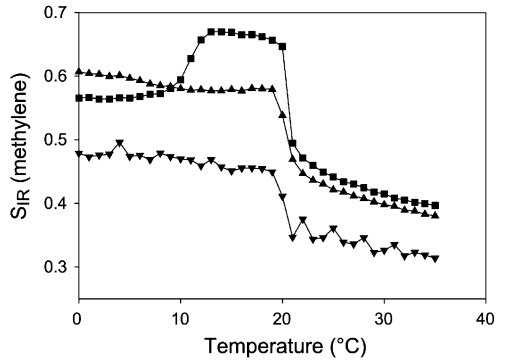

Figure 3. FTIR average order parameters of the methylene signals in pure DMPC chains (■), DMPC chains in the presence of ras at a molar ratio of 10:1 (▲), and the ras chains in the same preparation (▼). The data were acquired at full hydration (100% relative humidity).

Figure 3 shows IR order parameters of DMPC and of the ras lipid chains as a function of temperature. For pure DMPC bilayers this parameter exhibits two characteristic breakpoints which are assigned to the pretransition between the gel and the ripple gel phases and to the main transition between the ripple gel and the liquid crystalline phases, respectively. The pretransition clearly disappears in the presence of the ras peptide. The peptide obviously disturbs the packing of the lipid and thus prevents the formation of ripples. A perturbation of the arrangement of the lipid chains by the peptide can also be concluded from the respective chain order parameters. It is slightly smaller in the presence of the peptide in the ripple gel and liquid crystalline phases. At $T < 10$ °C, i.e., in the temperature range of the gel phase with tilted acyl chains of pure DMPC, the order parameter of the lipid acyl chains is, however, increased after addition of the peptide. This tendency is compatible with a decreased mean tilt angle of the acyl chain axes with respect to the membrane normal, which provides further indication of a perturbed packing mode of the myristoyl

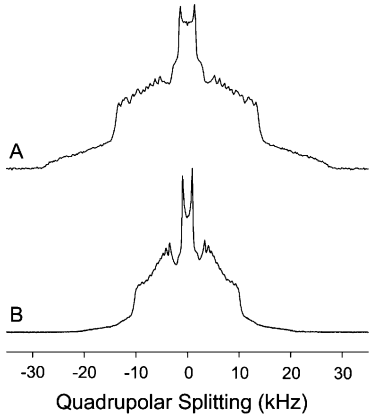

Figure 4. ^{2}H NMR spectra of DMPC-d_{54}/ras (A) and DMPC/ras-d_{66} (B) multilamellar vesicles. The lipid:peptide molar ratio was 10:1. Spectra were recorded at 30 °C and a water content of 30 wt %.

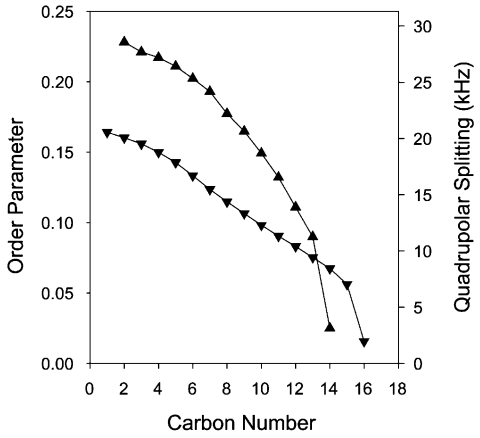

Figure 5. ^{2}H NMR order parameter profiles of the spectra shown in Figure 4 of the 14:0 DMPC-d_{54} (▲) and 16:0 ras-d_{66} (▼) lipid chains in multilamellar DMPC/ras liposomes (molar ratio 10:1) at a water content of 30 wt % and a temperature of 30 °C.

chains of the lipid after addition of the peptide. Note that the order parameter of the ras chains drops at the main phase transition of DMPC in accordance with the shift of the respective COG (see Figure 2).

Static ^{31}P NMR Spectra. According to the powder line shape of static ^{31}P NMR spectra (spectra not shown) and the anisotropy of the chemical shift, all investigated samples were in a lamellar liquid-crystalline phase state in both the absence and the presence of the ras peptide.

^{2}H NMR Order Parameters. In Figure 4, typical ^{2}H NMR powder spectra of the phospholipid chains in DMPC-d_{54}/ras (A) and the peptide chains in DMPC/ras-d_{66} (B) are shown. By switching the ^{2}H label between the DMPC and the ras chains, their order parameters can be studied individually. Much larger quadrupolar splittings are observed for the DMPC chains compared to the ras chains. For instance, the DMPC methyl groups exhibit a quadrupolar splitting of 3.1 kHz, while the methyl groups of the ras chains only show a quadrupolar splitting of 2.0 kHz. Similarly, the largest quadrupolar splitting measured for the DMPC C-2 methylene group is 28.5 kHz compared to only 20.5 kHz for the C-1 methylene groups of the ras hexadecyl chains. These changes are more instructively illustrated in the order parameter plots. In Figure 5, order parameters along the lipid chains of DMPC and ras are plotted. Significantly lower order parameters are obtained for the ras

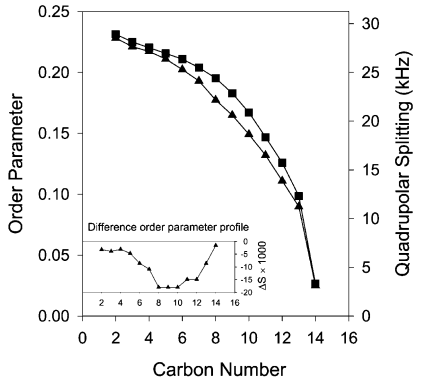

Figure 6. ^{2}H NMR order parameters of DMPC-d_{54} multilamellar liposomes in the absence (■) and presence (▲) of ras at a water content of 30 wt % and a temperature of 30 °C. The DMPC:ras molar ratio was 10:1. Inset: Difference order parameters obtained by subtracting the DMPC order parameters in the presence of ras from the order parameters in the absence of ras.

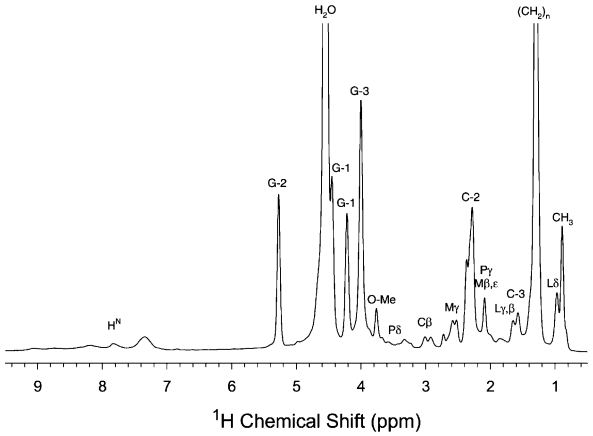

Figure 7. ^{1}H MAS NMR (600.1 MHz) spectrum of DMPC-d_{67}/ras in multilamellar vesicles at a molar ratio of 10:1. The sample was prepared at a water content of 30 wt %. The spectrum was acquired at a MAS spinning speed of 12 kHz and a temperature of 37 °C. Assignment of lipid and peptide peaks according to random coil chemical shifts is indicated.

chains compared to the DMPC chains, indicating that the ras chains must be more reduced in length compared to the DMPC chains.

^{2}H order parameters of DMPC in the absence and presence of ras are shown in Figure 6. In agreement with the FTIR data, a small decrease in order is observed in the presence of the ras peptide. To quantify order changes along the lipid chains, a difference order plot is shown in the inset of Figure 6. Peptide insertion leads to a decrease in order especially in the lower chain half. Such order changes are consistent with an interface location of the peptide moiety (see the Discussion).

^{1}H MAS NMR Measurements. In Figure 7, a 600.1 MHz ^{1}H MAS spectrum of DMPC-d_{67}/ras at a molar ratio of 10:1 is shown. Besides the dominating water, glycerol (G-1, G-2, and G-3), and lipid chain (CH_3, $(CH_2)_n$, C-2, and C-3) signals, resonance lines of the ras peptide are observed in the spectrum. Peak assignment of these peptide signals according to random coil values from the literature is given in the graph.[57] Peptide side chain signals show a typical line width of ≤0.1 ppm, which is comparable to that of phospholipids signals (~0.5 ppm). The

(57) Wishart, D. S.; Bigam, C. G.; Holm, A.; Hodges, R. S.; Sykes, B. D. *J. Biomol. NMR* **1995**, *5*, 67−81.

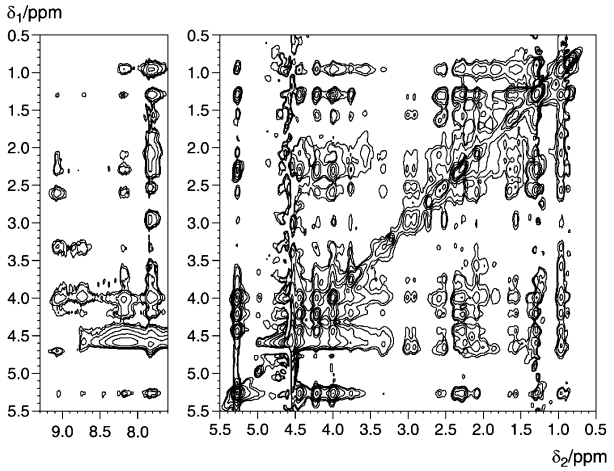

Figure 8. ^{1}H MAS NOESY (600 MHz) spectrum of DMPC-d_{67}/ras multilamellar vesicles at a mixing ratio of 10:1, a water content of 30 wt %, and a temperature of 37 °C. The spectrum was acquired at a MAS spinning speed of 12 kHz and a mixing time of 200 ms in a total acquisition time of approximately 15 h. All cross-peaks have positive intensity.

H^α protons cannot be observed because the spectral region between 3 and 4 ppm is dominated by the phospholipid glycerol signals. However, a signature of the peptide backbone is given through the MeO and the H^N signals, the latter showing a typical line width of ≤0.3 ppm.

The resolution of the 1D NMR spectrum allows the detection of spatial correlations by 2D MAS NOESY. In lipid/peptide NOESY spectra, typically three types of cross-peaks can be observed: (i) intramolecular peptide−peptide cross-peaks, (ii) intermolecular peptide−lipid cross-peaks, and (iii) exchange cross-peaks of the labile H^N protons with the solvent. In this study, we focus on the intermolecular lipid−peptide correlations, but we note that all types of cross-peaks are observed in the NOESY spectra.

In Figure 8, the aliphatic and amide regions of a MAS NOESY spectrum with a mixing time of 200 ms are shown. A number of strong cross-peaks of all three classes with positive intensity are found. Very strong exchange signals of the H^N protons with water are detected in agreement with the FTIR results, indicating that the peptide backbone has access to the aqueous phase. Also, there are intramolecular peptide−peptide correlations that provide structural information. It is beyond the scope of the present paper to analyze these intramolecular peptide cross-peaks for structure determination. This task requires isotopic labeling for ^{13}C editing of NOESY spectra, which is the subject of an upcoming study. In this paper, we restricted data analysis to the location of the polypeptide chain by analyzing intermolecular lipid−peptide cross-peaks.

Quantitative cross-peak analysis in lipid/peptide systems without isotopic labeling is challenging due to signal superposition and dynamic range problems. Therefore, we investigated the ras peptide in an almost fully deuterated DMPC-d_{67} matrix to attenuate the very intense phospholipid signals and highlight the peptide resonances. For the localization of the polypeptide chain parallel to the bilayer normal, cross-relaxation rates of peptide signals with signals from the methylene groups of the middle chain [$(CH_2)_n$], CH_2 groups of the upper chain (C-3, C-2), and the glycerol backbone (G-1, G-2, G-3) were calculated according to eq 3 and are shown in Figure 9. Because of signal superposition, only a few representative signals can be unam-

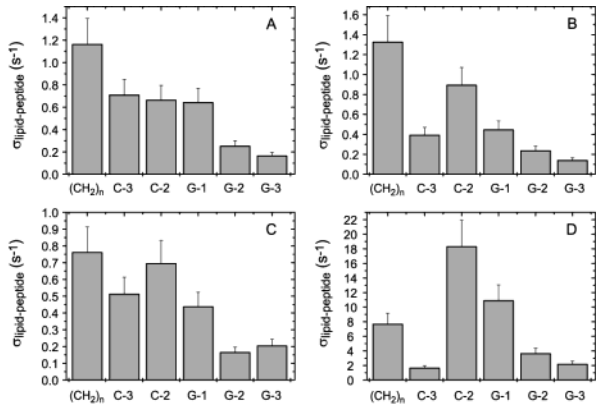

Figure 9. Quantitative analysis of intermolecular cross-peaks of the NOESY spectrum shown in Figure 8. Cross-relaxation rates reporting the transfer of magnetization from peptide to lipid signals of the middle chain [$(CH_2)_n$], the upper chain (C-3, C-2), and the glycerol backbone (G 1, G-2, G-3) were determined according to eq 2[46] for the Leu H^{δ} signals (A), the Met H^{γ} signels (B), the Cys H^{β} signals (C), and the amide H^N signal at 7.8 ppm (D).

biguously analyzed. All hydrophobic side chains (Leu H^{δ}, Met H^{γ}, and Cys H^{β}) show strong cross-relaxation rates with the middle and upper chain region of the lipid chains. Since cross-relaxation rates are proportional to the interaction strength between lipid and peptide segments and provide a measure for their contact probability,[46,58] it can be concluded that these side chains insert into the hydrocarbon core of the membrane. In contrast, the peptide backbone represented by the H^N protons at 7.8 ppm shows the strongest cross-relaxation rates with the upper chain/glycerol region of the bilayer, indicating an interface location of the peptide backbone.

It should be noted that cross-relaxation rates determined from a single NOESY experiment have a higher potential for errors than rates determined from NOESY spectra acquired as a function of mixing time.[46] This approach, however, is not feasible with this sample as a single spectrum already requires a measuring time of almost 15 h. Using ^{13}C-labeled ras peptide would overcome signal superposition with phospholipid resonances and sensitivity problems of the simple $^1H-^1H$ NOESY. Nevertheless, it is possible to conclude from the current data set that the peptide backbone is localized at the lipid−water interface of the membrane and that the hydrophobic side chains are more deeply inserted into the phospholipid acyl chain region.

The influence of spin diffusion in these NOESY measurements can be neglected for intermolecular cross-relaxation if the mixing time is kept short as in our experiments.[59]

Neutron Diffraction. In Figure 10, neutron scattering length density profiles of DMPC-d_{54} in the absence and presence of ras (10:1 molar ratio) are shown. This sample was prepared with a relative humidity of 100% (full hydration). Three equidistant Bragg peaks were detected and converted into the low-resolution density profiles shown. The neutron scattering length density profiles of DMPC-d_{54} in the absence and presence of ras agree relatively well in the headgroup and glycerol region of the bilayer. However, significant alterations are observed in the acyl chain region where lower scattering is observed in the presence of ras. These results can be interpreted by assuming that the protonated ras lipid chains insert into the membrane, thereby

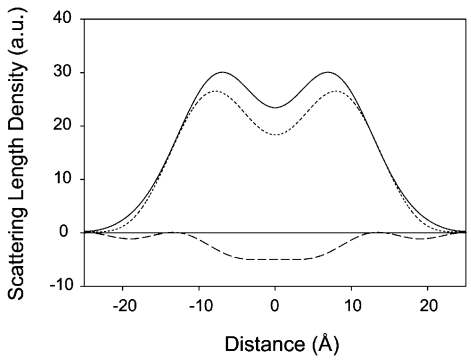

Figure 10. Relative neutron scattering length density profile of DMPC-d_{54} in the absence (solid line) and presence (dotted line) of ras at a DMPC-d_{54}/ras molar ratio of 10:1. The profiles were calculated from neutron diffraction data (Bragg reflexes up to the third order) obtained at a relative humidity of 100% H_2O and a temperature of 30 °C. The difference between the two profiles is shown as a dashed line. Fourier coefficients: DMPC-d_{54}, +6.00, −1.45, −1.37, −0.28; DMPC-d_{54}/ras, +7.66, −2.92, −2.18.

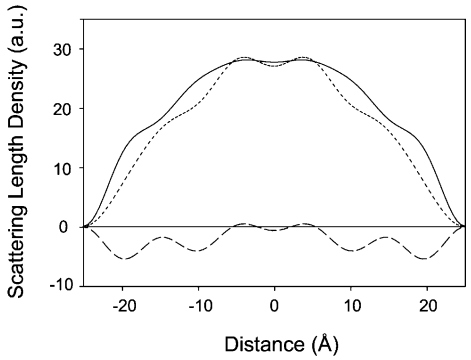

Figure 11. Relative neutron scattering length density profile of DMPC-d_{67} in the absence (solid line) and presence (dotted line) of ras-d_{66} at a DMPC-d_{67}/ras-d_{66} molar ratio of 10:1. The profiles were calculated from neutron diffraction data (Bragg reflexes up to the sixth order) obtained at a relative humidity of 98% H_2O and a temperature of 30 °C. The difference between the two profiles is shown as a dashed line. Fourier coefficients: DMPC-d_{67}, +7.81, −2.28, +0.98, −1.14, +0.67, −0.34; DMPC-d_{67}/ras-d_{66}, +8.52, −1.46, +0.90, −0.67, −0.44, −0.24.

diluting the density of the deuterated acyl chains of the phospholipids, resulting in a decrease in scattering length density. The variations in the headgroup/glycerol area are due to the peptide backbone and side chains that vary the scattering length density toward the phospholipids. This region is explored in more detail in the DMPC-d_{67}/ras-d_{66} experiments shown below.

The insertion depth and distribution of the protonated ras lipid chains can be determined from the difference of the neutron scattering length density profiles in the presence and absence of ras as shown in Figure 10 as a dashed line. Therefore, the ras lipid chains are located in the middle of the lipid membrane and extend approximately ±10 Å from the bilayer center, which agrees well with the thickness of the hydrophobic region of the DMPC membrane, where the acyl chains are located.

To investigate the distribution of the peptide backbone and side chains, neutron diffraction patterns were collected on mixtures of DMPC-d_{67} and ras-d_{66}. In this preparation, the contrast variation is due to the protonated peptide residues. To improve the resolution of the scattering length density profile, samples were hydrated to only 98% relative humidity. Under these conditions, six equidistant Bragg reflexes were observed,

(58) Feller, S. E.; Brown, C. A.; Nizza, D. T.; Gawrisch, K. *Biophys. J.* **2002**, *82*, 1396−1404.
(59) Huster, D.; Gawrisch, K. *J. Am. Chem. Soc.* **1999**, *121*, 1992−1993.

increasing the nominal resolution from 19 to 8.5 Å in the neutron scattering length density profiles[52,60] shown in Figure 11.

The displayed scattering length density profiles of DMPC-d_{67} in the absence and presence of ras-d_{66} show significant alterations in the headgroup/glycerol/upper chain region, which is commonly referred to as the lipid−water interface of the membrane. Again, information about distribution and insertion depth is most easily extracted from the difference scattering length density plots as shown in Figure 11. Due to the different contrast in neutron scattering length density present, the profiles coincide in the bilayer center but significant alterations are obtained at the lipid−water interface. Two broad distribution peaks are detected about ±10 and ±19 Å from the bilayer center. These areas indicate regions of the bilayer where the deuterated phospholipid matrix is diluted with the protonated peptide backbone and amino acid side chains, resulting in lower neutron scattering length densities in the lipid−water interface of the membrane.

Discussion

The C-terminus of the human N-ras protein contains two lipid modifications, a farnesyl chain and a palmitoyl chain, that provide a membrane anchor for the protein. In this study, we have investigated membrane binding of a heptapeptide with the amino acid sequence of the C-terminus of N-ras carrying two lipid modifications. The farnesyl chain was replaced by a hexadecyl thioester to avoid signal superposition in ^{1}H NMR spectra and to introduce the possibility to deuterate that chain. It has been shown that replacement of the farnesyl chain in H-ras by various farnesyl analogues of similar chain length had no impact either on the palmitoylation of the protein or on the downstream regulation.[61]

With these unpolar lipid anchors, the peptide gains substantially in hydrophobicity, providing the driving force for membrane insertion. Energetically, insertion of each CH_2 group from aqueous solution into a nonpolar environment contributes 0.825 kcal/mol of hydrophobic energy,[62] which has also been experimentally confirmed for lipid-modified peptides.[15,17,63] For the ras peptide with two 16:0 chains this amounts to more than 20 kcal/mol, explaining the high propensity of the peptide for the membrane.

Ras Lipid Chain Insertion. There are several lines of evidence that the peptide lipid chains insert into the DMPC host matrix.

First, FTIR measurements revealed that the phospholipid and peptide chains undergo their phase transition at exactly the same temperature (Figure 2). Therefore, the peptide chains are immersed in the DMPC membrane and not sequestered into separate domains. For sensitivity reasons, it was necessary to mix the peptide at a 1:10 molar ratio with the lipids. While it is desirable to work with dilute systems, the high peptide concentration did not lead to a multimer formation. Appropriate isotopic labeling will allow the peptide-to-lipid ratio to be further decreased.

Second, peptide chain order parameters are much smaller than those of the phospholipids. This is seen from FTIR experiments (Figure 3) and with much better chain resolution from ^{2}H NMR (Figure 5). By switching the ^{2}H label between the DMPC and ras lipid chains, individual order parameters for each chain can be obtained. From ^{2}H NMR measurements at 30 °C, the average order parameter of the DMPC chains is 0.167 while the average order parameter of the ras chains is 0.110. The effective length of a saturated hydrocarbon chain is proportional to the average order parameter.[64] Therefore, the order parameters can be converted into an average chain length of the DMPC and ras chains. At 30 °C, the DMPC chains are 11.0 Å long while the ras chains have an average length of 11.6 Å. This explains why the ras chains have such low order parameters. In an ideal mixture of DMPC and ras chains, the average chain lengths should be identical. Since the ras 16:0 chains are two methylene groups longer than the 14:0 DMPC chains, they decrease their order upon membrane insertion to match the chain length of the host lipids.

The order and dynamics of the fatty acid chain in 16:0-lipid-modified gramicidin were previously studied.[65] A much different order parameter profile was obtained showing very low order for the upper chain. This translated to a difference of 2.1 Å between peptide and lipid chains. This was interpreted as a bend that the helical gramicidin peptide forced in the acyl chain near the carboxyl terminus of the peptide where the palmitoyl chain was attached. The perfect peptide chain insertion observed for the ras peptide in this study suggests that the peptide structure is flexible, allowing the chains to freely associate with the phospholipid acyl chains.

Third, from neutron scattering experiments, the distribution of the ras peptide chains was determined by proton/deuteron contrast variation (Figure 10). As expected, the ras lipid chains are localized in the hydrophobic interior of the membrane identical to the phospholipid acyl chains of the DMPC host matrix.

Several studies of membrane insertion of lipidated peptides or proteins are found in the literature. For instance, it was concluded that only about 10 CH_2 groups of the myristoylated src peptide penetrate the hydrocarbon interior of the membrane.[19,22] The src peptide belongs to the group of peptides that bind the membrane via a combination of one fatty acid modification and a cluster of basic amino acid residues. For the charged amino acids of the peptide it is impossible to overcome the Born repulsion that comes about when a polar molecule approaches a low dielectric environment.[10,66] Therefore, incomplete insertion of the myristoyl fatty acid chain occurs, and the energetically unfavorable exposure of the upper myristoyl chain is tolerated.

Similarly, it has been concluded from binding studies of myristoylated or palmitoylated bovine pancreatic trypsin inhibitor (BPTI) that about 3.4 methylene groups are prevented from partitioning into the bilayer.[63] These authors suggest that steric interference and membrane dehydration due to the close contact between the membrane surface and the protein prevent the entire acyl chain from partitioning.

(60) Franks, N. P.; Lieb, W. R. In *Liposomes: From Physical Structure to Therapeutic Applications;* Knight, C. G., Ed.; Elsevier/North-Holland: Amsterdam, 1981; pp 243−272.
(61) Dudler, T.; Gelb, M. H. *Biochemistry* **1997**, *36*, 12434−12441.
(62) Tanford C. *The hydrophobic effect: formation of micells and biological membranes*; John Wiley & Sons: New York, 1980.
(63) Pool, C. T.; Thompson, T. E. *Biochemistry* **1998**, *37*, 10246−10255.
(64) Nagle, J. F. *Biophys. J.* **1993**, *64*, 1476−1481.
(65) Vogt, T. C.; Killian, J. A.; de Kruijff, B. *Biochemistry* **1994**, *33*, 2063−2070.
(66) Ben-Tal, N.; Honig, B.; Peitzsch, R. M.; Denisov, G.; McLaughlin, S. *Biophys. J.* **1996**, *71*, 561−575.

Contrary to these results, in our experiments we see a full insertion of the ras hydrocarbon chains into the DMPC membrane. The ras peptide carries no fixed charges, and the Born repulsion is of much smaller magnitude compared to that of the highly charged src peptide. Therefore, the flexible polypeptide chain can approach and penetrate the membrane surface without major repulsion, allowing the hydrocarbon chains of the peptide to assume a low-order configuration. Consequently, the physicochemical properties of the ras hydrocarbon chains are found similar to those of the DMPC host matrix.

It should be noted that cellular membranes are constituted of lipids with 16−20 carbon chains, some of which are unsaturated. While unsaturated lipids are not available with the varying degrees of deuteration necessary for this study, we note that the lipid chain length of unsaturated lipids is better represented by DMPC than by saturated lipids with longer chains, which also have a higher main phase transition temperature that would require the experiments to be carried out at higher temperature.

Localization of the Peptide Backbone and Side Chains. If the ras hydrocarbon chains insert completely into the membrane interior and approximately match the length of the myristoyl chains of the DMPC host matrix, one should expect that the peptide backbone would be located in the glycerol/headgroup region of the membrane. Indeed this has been confirmed by several experimental techniques employed in this study. Therefore, the question arises of how deep the polypeptide chain enters the bilayer.

The most precise and quantitative information about peptide penetration into the lipid membrane comes from the ^{1}H MAS NOESY results since the method detects the interaction strength between lipid and peptide segments. These measurements allow individual amino acid side chains and the peptide backbone in the bilayer to be quantitatively localized. Measuring the interaction strength between lipid and peptide segments, it could be shown that the hydrophobic side chains of Leu, Met, and Cys penetrate the upper and middle chain region of the bilayer while the peptide backbone is located closer to the aqueous phase (Figure 9). This agrees with the distribution profiles obtained from neutron diffraction experiments and allows a more quantitative assessment of the location of individual amino acids of the peptide.

The NOESY results are consistent with the experimentally determined hydrophobicity scale by Wimley and White.[67] The most hydrophobic side chains in the peptide sequence are Leu and Cys. According to the NOESY data, these side chains show strong magnetization exchange with upper and middle chain segments (Figure 9), indicating that they insert deeply into the bilayer. Also, the Cys side chains have the largest cross-relaxation rates with the upper and middle chain segments. This is consistent with the assumption that insertion of the peptide's lipid chains drags the Cys side chains deeper into the nonpolar lipid chain phase, where these side chains interact favorably with upper acyl chain segments. The most hydrophilic side chain according to the hydrophobicity scale is Pro, while the Gly residues only contribute a vanishing free energy of transfer. Unfortunately, due to superposition with peptide or lipid glycerol and fatty acid signals no unambiguous assignment of Pro and Gly cross-peaks can be made at the moment. This will be possible with ^{13}C labeling of the amino acids, which is under investigation. If all amino acid contributions are added up, a total free energy of transferring the peptide from water to the lipid bilayer of −0.8 kcal/mol is calculated. This is a relatively small contribution compared to the ∼−20 kcal/mol hydrophobic energy contributed from the chain methylenes but supports the high propensity of the ras peptide for the membrane environment.

The good resolution of the ^{1}H MAS spectra suggests that the peptide is highly dynamic and flexible in the lipid membrane and perhaps even undergoes axially symmetric reorientations similar to the phospholipid molecules. Such motions are necessary to scale down the strong homonuclear ^{1}H−^{1}H dipolar couplings that are on the order of 40 kHz in rigid solids. MAS of only 12 kHz would not be sufficient to average out the homogeneous dipolar tensor,[68] and the resolved ^{1}H MAS spectra indicate the result of the peptide's mobility.

The other methods corroborate the conclusions about the location of the ras peptide in the lipid−water interface of the membrane defined by the upper chain/glycerol/headgroup region.[69−73] Neutron scattering length density profiles of ras-d_{66} in DMPC-d_{67} provide an experimentally determined distribution function of the polypeptide chain in the membrane (Figure 11). The widths of these distributions are broad as in the NOESY data. In accordance with the NOESY results it is tempting to suggest that the two peptide distribution maxima are due to the peptide backbone and hydrophobic side chains. However, the current resolution of the neutron scattering length density profiles does not allow such a strict distinction. In fact the nominal resolution determines the half-width of the density peaks, whereas the peak location can be determined with an error of ∼2 Å (at 8.5 Å resolution).[74,75]

Nevertheless, the data show that a significant portion of the peptide must penetrate the upper chain region of the bilayer while part of the peptide is also localized in the headgroup region of the membrane. This region of maximal peptide insertion coincides with the onset of the drop of molecular order observed for the DMPC chains in the presence of the ras peptide (Figure 6).

Further support for the structural model of the membrane-bound ras peptide comes from both FTIR and ^{1}H MAS NMR, indicating that the labile amide protons are in fast exchange with water. This suggests that the peptide backbone must be located not too far from the membrane surface, where water molecules still penetrate the membrane. This is only fulfilled for the lipid−water interface of the membrane.

Finally, the ^{2}H NMR results are also in agreement with location of the polypeptide chain in the membrane. In the presence of the peptide, the DMPC order parameters are decreased. The order parameter decrease is more pronounced in the lower part of the acyl chains (Figure 6). This is consistent

(67) Wimley, W. C.; White, S. H. *Nat. Struct. Biol.* **1996**, *3*, 842−848.
(68) Davis, J. H.; Auger, M.; Hodges, R. S. *Biophys. J.* **1995**, *69*, 1917−1932.
(69) Simon, S. A.; McIntosh, T. J. *Methods Enzymol.* **1986**, *127*, 511−521.
(70) Gawrisch, K.; Ruston, D.; Zimmerberg, J.; Parsegian, V. A.; Rand, R. P.; Fuller, N. *Biophys. J.* **1992**, *61*, 1213−1223.
(71) Armen, R. S.; Uitto, O. D.; Feller, S. E. *Biophys. J.* **1998**, *75*, 734−744.
(72) Marrink, S.-J.; Berendsen, H. J. C. *J. Phys. Chem.* **1994**, *98*, 4155−4168.
(73) Huster, D.; Jin, A. J.; Arnold, K.; Gawrisch, K. *Biophys. J.* **1997**, *73*, 855−864.
(74) Büldt, G.; Gally, H. U.; Seelig, J.; Zaccai, G. *J. Mol. Biol.* **1979**, *134*, 673−691.
(75) Hauss, T.; Grzesiek, S.; Otto, H.; Westerhausen, J.; Heyn, M. P. *Biochemistry* **1990**, *29*, 4904−4913.

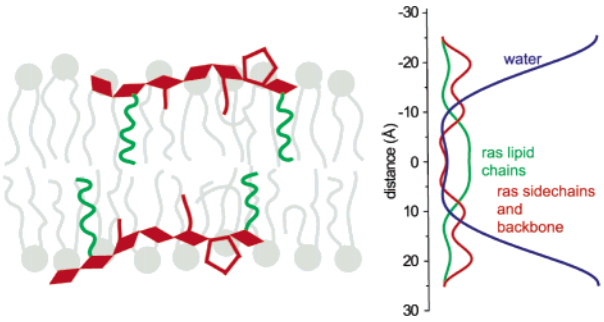

Figure 12. Structural results for membrane insertion of the lipid-modified ras peptide from this study. The peptide backbone is dynamically distributed in the lipid−water interface of the membrane. Hydrophobic peptide side chains insert into the interior of the membrane, while the Pro side chain is most likely facing the aqueous phase. The peptide lipid chains are more disordered than the phospholipid chains to match the average length of the DMPC acyl chains of the host membrane. The peptide backbone is in exchange with water that penetrates the membrane to the interface region. On the right-hand side, distribution functions of water (blue), ras lipid chains (green), and amino acid residues (red) as determined from the neutron diffraction experiments are shown.

with an interfacial location of the polypeptide chain. Insertion of the peptide leaves the upper chain segments basically unchanged but leads to a lower lipid packing density, providing the lower acyl chain regions more motional freedom, which decreases order. From the difference order parameter plot (Figure 6) one can roughly estimate that the peptide must enter the acyl chain region of DMPC up to the fourth to sixth carbon. The sudden drop of order indicates the increased free volume in the lower half of the bilayer coinciding with the maximum of the peptide side chain location determined by neutron diffraction (Figure 11). However, inferring the depth of peptide penetration from order parameter profiles only is risky and can only support methods such as ^{1}H MAS NOESY or neutron diffraction.

All the experimental results of this study support a model of the lipidated ras peptide binding to the membrane as illustrated in Figure 12. The peptide hydrocarbon chains are fully inserted into the hydrophobic core of the membrane and are more disordered than the phospholipid chains. Thus, they match closely the average length of the DMPC acyl chains. The peptide backbone is localized at the lipid−water interface of the membrane and subject to a broad dynamic distribution. Hydrophobic peptide side chains are also dynamically distributed and insert deeper into the hydrophobic membrane center. The more hydrophilic Pro is likely to face the aqueous phase. The peptide backbone is in fast exchange with water that penetrates the membrane at the interface region. On the right-hand side of Figure 12, the distribution functions of water (blue), ras lipid chains (green), and amino acid residues (red) as determined from the neutron diffraction experiments are shown.

Conclusions

Contrary to charged lipidated peptides, the polypeptide chain of the doubly lipid modified peptide derived from the carboxyl terminus of the human N-ras protein is located at the lipid−water interface of the membrane. The peptide lipid chains insert completely into the phospholipid acyl chain region, maximizing the hydrophobic interactions. Peptide and phospholipid chains have very similar physicochemical properties. Hydrophobic amino acid side chains also penetrate the middle chain region and contribute their binding energy to a free energy minimum of the lipid/peptide complex. Signatures of a defined peptide secondary structure were not found. Therefore, the peptide is assumed to have a flexible structure in the bilayer and experiences large conformational freedom. Consequently, the location of the peptide segments is described by broad distribution functions parallel to the membrane normal. Since the C-terminus of the ras protein is unstructured,[30,33] the described mobile peptide conformation appears to be relevant for the structure of the full-length membrane-bound ras protein.

Acknowledgment. The work was supported by the Deutsche Forschungsgemeinschaft (Ar 195/8-1) and the Saxon State Ministry of Higher Education, Research and Culture (Junior Research Group "Solid-state NMR Studies of Membrane-associated Proteins"). D.H. thanks Dr. Klaus Gawrisch and David Nizza for valuable discussions about quantitative cross-peak integration.

JA0289245